Electronic Supplementary Material (ESI) for Physical Chemistry Chemical Physics.
This journal is © the Owner Societies 2017

Electronic supplementary information (ESI)

For

Phase transformations, anisotropic pyroelectric energy harvesting and electrocaloric properties of (Pb,La)(Zr,Sn,Ti)O_3 single crystals

Fangping Zhuo[a], Qiang Li*[a], Jinghan Gao[a], Qingfeng Yan[a], Yiling Zhang[b], Xiaoqing Xi[b] and Xiangcheng Chu[b]

[a]*Department of Chemistry, Tsinghua University, Beijing 100084, China. E-mail: qiangli@mail.tsinghua.edu.cn. Fax: +86-10-62771179; Tel: +86-10-62797871*

[b]*State Key Laboratory of New Ceramics and Fine Processing, Tsinghua University, Beijing 100084, China*

1. Electric field induced phase transition

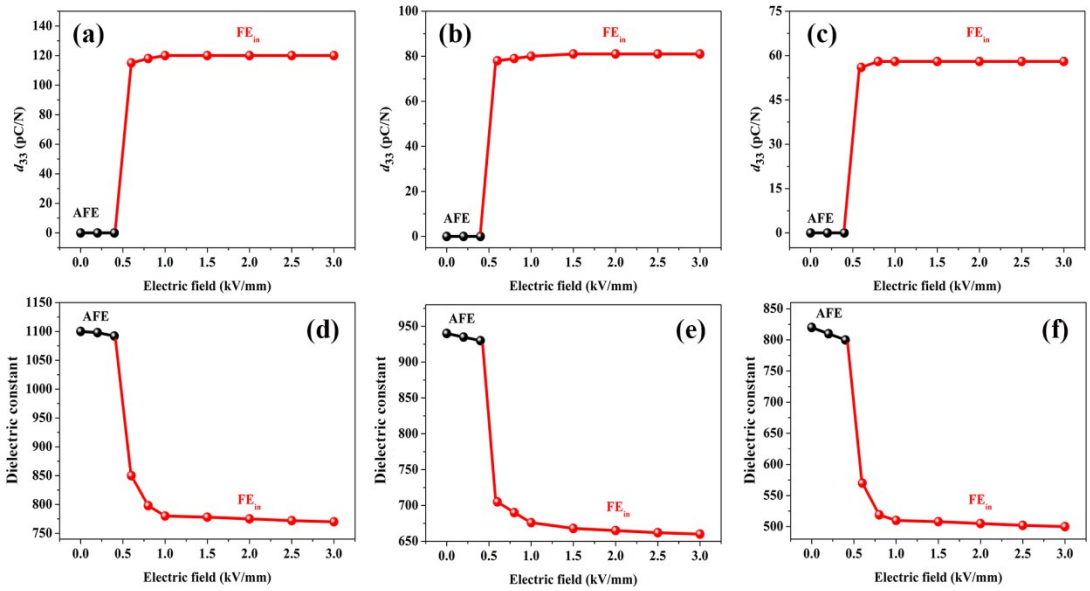

Fig. S1 The piezoelectric coefficients d_{33} as a function of the poling electric field for (a) [100]-, (b) [110]- and (c) [111]-oriented PLZST single crystals. The corresponding dielectric constant as a function of the poling electric field for (d) [100]-, (e) [110]- and (f) [111]-oriented PLZST single crystals. The AFE phase is a

nonpolar state, so that no piezoelectric coefficient can be detected.[1] However, the FE phase is a polar state and the piezoelectric coefficient can be measured. The dielectric constant decreases sharply at the tetragonal AFE to rhombohedral FE phase transition critical electric field. The piezoelectric and dielectric properties also confirm the tetragonal AFE to rhombohedral FE phase transition during the poling process.

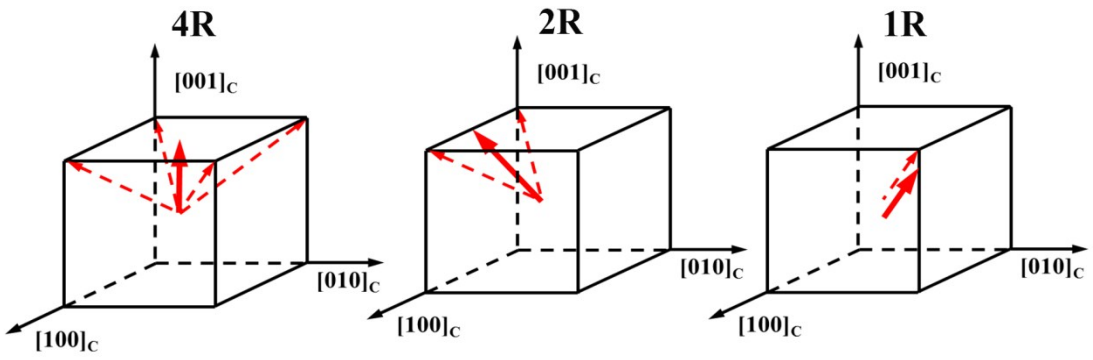

Fig. S2 The engineered domain configurations of the rhombohedral FE phase. Different engineered domain configurations 1R, 2R and 4R can be realized by poling the crystals along [111], [110] and [001] crystallographic directions. The solid arrow is the applied electric field direction.

2. Temperature driven phase transition

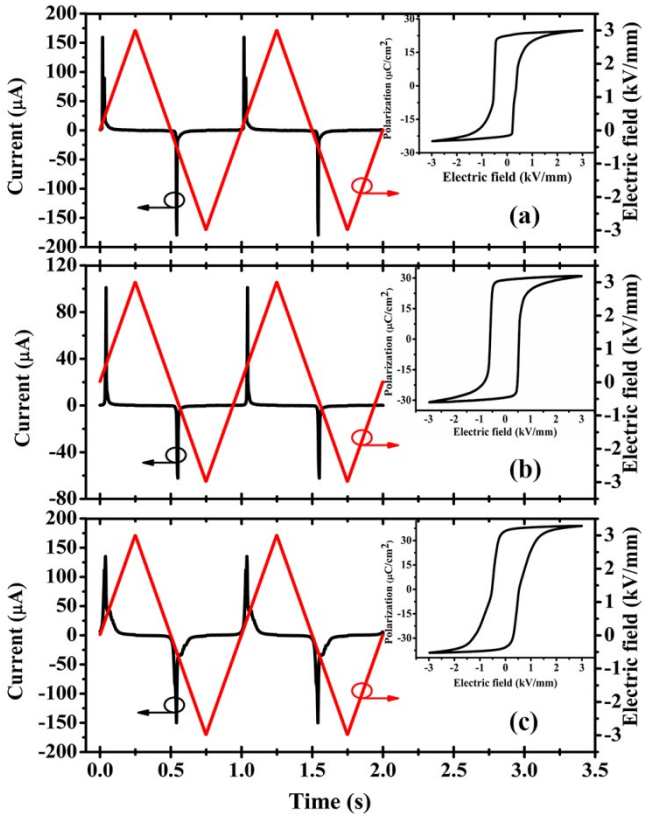

Fig. S3 Current response to electric field stimulus at room temperature for (a) [100]-, (b) [110]-, (c) [111]-oriented PLZST crystals, respectively. The inset shows the corresponding *P*–*E* loop.

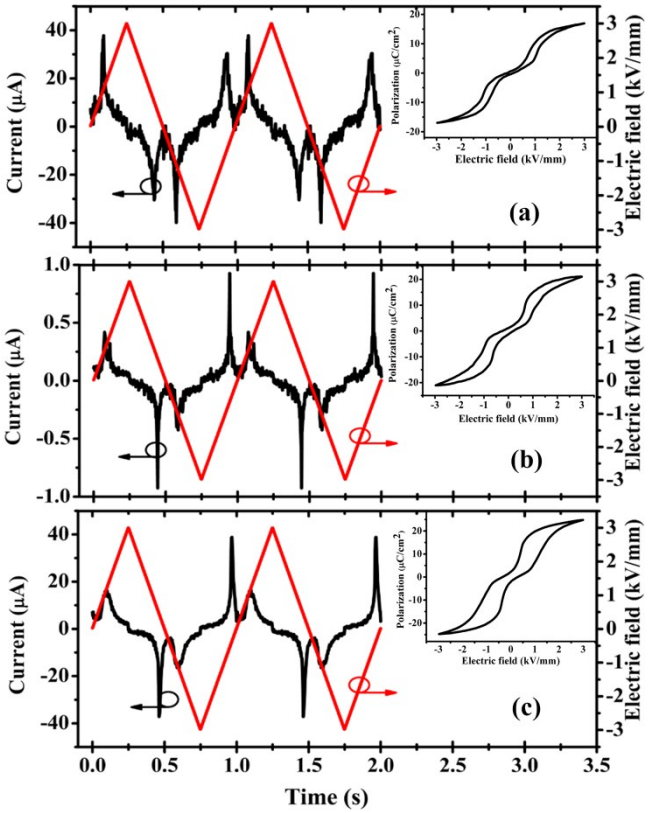

Fig. S4 Current response to electric field stimulus at 150 °C for (a) [100]-, (b) [110]-, (c) [111]-oriented PLZST crystals, respectively. The inset shows the corresponding *P*–*E* loop.

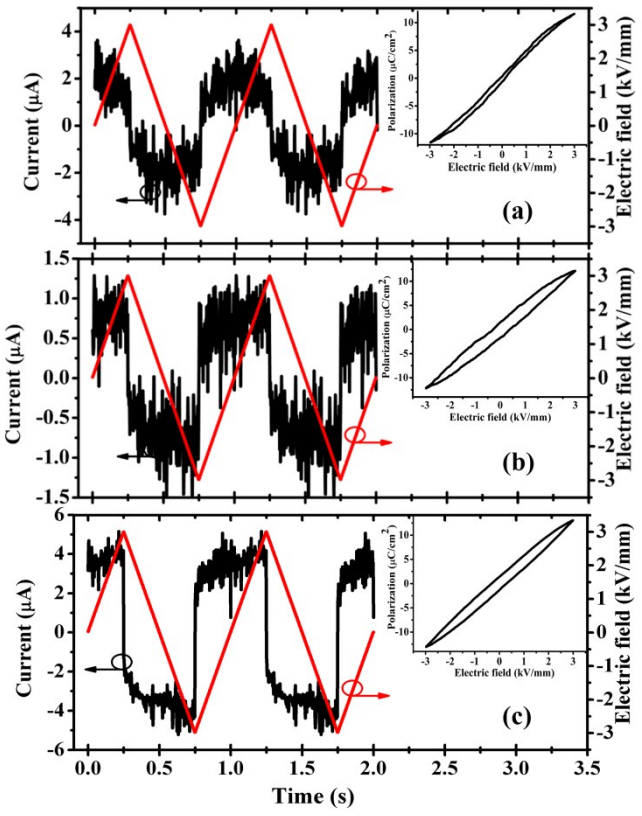

Fig. S5 Current response to electric field stimulus at 180 °C for (a) [100]-, (b) [110]-, (c) [111]-oriented PLZST crystals, respectively. The inset shows the corresponding *P*–

E loop.

At room temperature, typical FE polarization switching behaviors are observed, as shown in Fig. S**3**. It can be seen that the electric field induced FE phase is similar to normal or relaxor ferroelectrics.[2-4] When temperature is above T_d, typical AFE polarization switching processes are found. As shown in Fig. S**4**, all samples display typical AFE double *P*–*E* loop with four current peaks in the current–time curves per cycle. With further increasing the temperature, typical PE current–time curves are obtained (see Fig. S**5**). The current response to electric field stimulus at selected temperatures also reveals the FE_{in}–AFE–PE phase transitions sequence.

3. Ferroelectric and antiferroelectric phase structure.

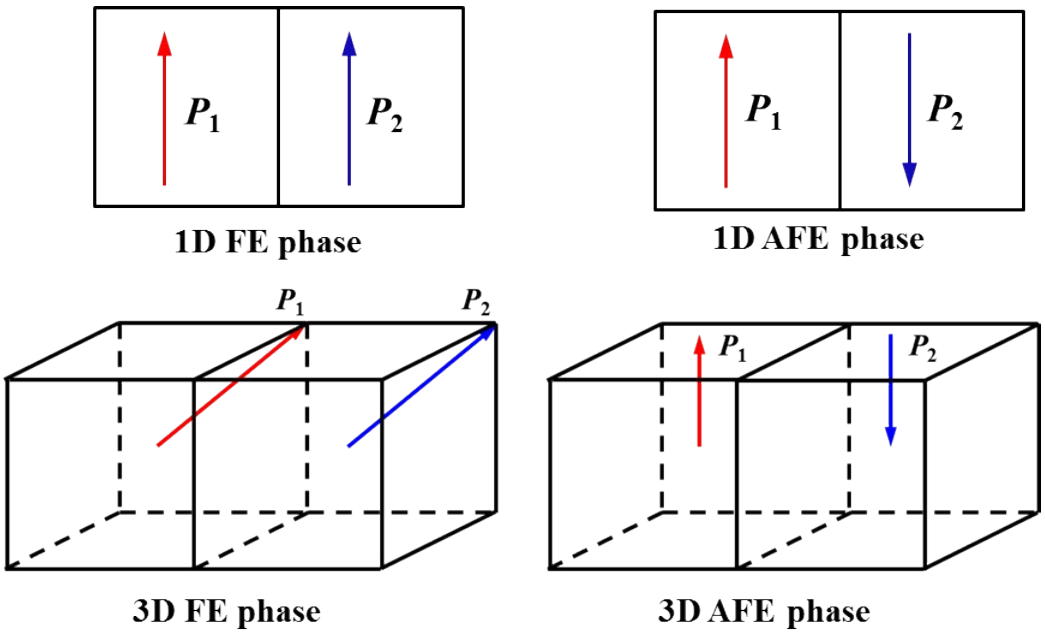

Fig. S6 Schematic plot of the one-dimensional (1D) and three-dimensional (3D) AFE

and FE phases. Note that the PLZST crystal is divided into two sublattices, 1 and 2, associated with polarizations P_1 and P_2, respectively. If P_1 and P_2 are antiparallel to each other, the system exhibits the AFE phase.[5,6] On the other hand, it is the FE phase if P_1 and P_2 are parallel to each other.

4. Anisotropy of energy harvesting and electrocaloric effect

In order to understand the anisotropy of ECE behaviors, the ΔT for the PLZST crystal with [100] orientation can be given as

$$\Delta T_{[100]} = T \exp\left\{\frac{a_0 \sum_{i=1}^{2} [P_{[100],i}^2(0,T) - P_{[100],i}^2(E,T+\Delta T)]}{C_{\text{ph}}}\right\} - T \tag{S1}$$

For the PLZST crystal with [110] orientation, we have

$$\Delta T_{[110]} = T \exp\left\{\frac{a_0 \sum_{i=1}^{2} [P_{[110],i}^2(0,T) - P_{[110],i}^2(E,T+\Delta T)]}{C_{\text{ph}}}\right\} - T \tag{S2}$$

For the PLZST crystal with [111] orientation, we obtain

$$\Delta T_{[111]} = T \exp\left\{\frac{a_0 \sum_{i=1}^{2} [P_{[111],i}^2(0,T) - P_{[111],i}^2(E,T+\Delta T)]}{C_{\text{ph}}}\right\} - T \tag{S3}$$

According to Eq. (16), we have

$$\Delta T_{[100]} = T \exp\left\{\frac{S_{[100],\text{dip}}(T,0) - S_{[100],\text{dip}}(T+\Delta T,E)}{C_{\text{ph}}(T)}\right\} - T \tag{S4}$$

$$\Delta T_{[110]} = T \exp\left\{\frac{S_{[110],\text{dip}}(T,0) - S_{[110],\text{dip}}(T+\Delta T,E)}{C_{\text{ph}}(T)}\right\} - T \tag{S5}$$

$$\Delta T_{[111]} = T \exp\left\{\frac{S_{[111],\text{dip}}(T,0) - S_{[111],\text{dip}}(T+\Delta T,E)}{C_{\text{ph}}(T)}\right\} - T \tag{S6}$$

Then, we have

$$\Delta T_{[100]} = T \exp\left\{\frac{\Delta S_{[100]}}{C_{\text{ph}}(T)}\right\} - T \tag{S7}$$

$$\Delta T_{[110]} = T \exp\left\{\frac{\Delta S_{[110]}}{C_{\text{ph}}(T)}\right\} - T \tag{S8}$$

$$\Delta T_{[111]} = T \exp\left\{\frac{\Delta S_{[111]}}{C_{\text{ph}}(T)}\right\} - T \tag{S9}$$

In order to understand the anisotropy of pyroelectric energy harvesting behaviors, the energy density for PLZST crystal can be given as[7]

$$W = (E_H - E_L) \times \{\frac{\varepsilon_0}{2}[\varepsilon_r(E, T_1) - \varepsilon_r(E, T_2)](E_H + E_L) + P_s(T_1) - P_s(T_2)\} \quad \text{(S10)}$$

where T_1 is the low temperature and T_2 is the high temperature, respectively. Then, we can write Eq. (S10) into Eq. (S11) as

$$W = (E_H - E_L) \times \{\Delta\varepsilon(E, \Delta T)(E_H + E_L) + \Delta P_s(\Delta T)\} \quad \text{(S11)}$$

For the present PLZST system, it is assumed that the dielectric contribution $W_\varepsilon = \Delta\varepsilon(E, \Delta T)(E_H^2 - E_L^2)$ is isotropy. Then, we give

$$W_{[100]} = W_\varepsilon + \Delta P_{[100],s}(\Delta T)\Delta E \quad \text{(S12)}$$

$$W_{[110]} = W_\varepsilon + \Delta P_{[110],s}(\Delta T)\Delta E \quad \text{(S13)}$$

$$W_{[111]} = W_\varepsilon + \Delta P_{[111],s}(\Delta T)\Delta E \quad \text{(S14)}$$

According to engineered domain configuration and measured temperature dependent *P*–*E* loops, we can deduce that $\Delta P_{[100],s} < \Delta P_{[110],s} < \Delta P_{[111],s}$ (see Fig. 6). Therefore, the energy harvesting density has a relationship followed by $W_{[100]} < W_{[110]} < W_{[111]}$. Actually, a large polarization change usually leads to a large entropy change, i.e.

$$\Delta P_{[100]}^2 \propto \Delta S_{[100]} \quad \text{(S15)}$$

$$\Delta P_{[110]}^2 \propto \Delta S_{[110]} \quad \text{(S16)}$$

$$\Delta P_{[111]}^2 \propto \Delta S_{[111]} \quad \text{(S17)}$$

Then, we have

$$W_{[100]} \propto \sqrt{\Delta S_{[100]}} \quad \text{(S18)}$$

$$W_{[110]} \propto \sqrt{\Delta S_{[110]}} \quad \text{(S19)}$$

$$W_{[111]} \propto \sqrt{\Delta S_{[111]}} \quad \text{(S20)}$$

References

1 F. P. Zhuo, Q. Li, J. H. Gao, Y. J. Wang, Q. F. Yan, Y. L. Zhang, X. Q. Xi, X. C. Chu and W. W. Cao, *Appl. Phys. Lett.*, 2016, 108, 082904.

2 A. F. Devonshire, *Adv. Phys.*, 1954, **3**, 85–130.

3 P. Yang and D. A. Payne, *J. Appl. Phys.*, 1992, **71**, 1361–1367.

4 F. P. Zhuo, Q. Li, J. H. Gao, Y. J. Wang, Q. F. Yan, Y. L. Zhang and X. C. Chu, *J. Am. Ceram. Soc.*, 2016, **99**, 2047–2054.

5 C. Kittel, *Phys. Rev.* 1951, **82**, 729–732.

6 K. Okada, *J. Phys. Soc. Jpn.*, 1969, **27**, 420–428.

7 F. Y. Lee, H. R. Jo, C. S. Lynch and L. Pilon, *Smart Mater. Struct.*, 2013, **22**, 025038.